

Unsymmetrical Bimetallic Complexes with $M^{II}-(\mu\text{-OH})-M^{III}$ Cores ($M^{II}M^{III} = \text{Fe}^{II}\text{Fe}^{III}, \text{Mn}^{II}\text{Fe}^{III}, \text{Mn}^{II}\text{Mn}^{III}$): Structural, Magnetic, and Redox Properties

Yohei Sano,[†] Andrew C. Weitz,[‡] Joseph W. Ziller,[†] Michael P. Hendrich,[‡] and A. S. Borovik^{*†}

[†]Department of Chemistry, University of California—Irvine, 1102 Natural Sciences II, Irvine, California 92697-2025, United States

[‡]Department of Chemistry, Carnegie Mellon University, Pittsburgh, Pennsylvania 15213, United States

Supporting Information

ABSTRACT: Heterobimetallic cores are important units within the active sites of metalloproteins but are often difficult to duplicate in synthetic systems. We have developed a synthetic approach for the preparation of a complex with a $\text{Mn}^{II}-(\mu\text{-OH})-\text{Fe}^{III}$ core, in which the metal centers have different coordination environments. Structural and physical data support the assignment of this complex as a heterobimetallic system. A comparison with analogous homobimetallic complexes, $\text{Mn}^{II}-(\mu\text{-OH})-\text{Mn}^{III}$ and $\text{Fe}^{II}-(\mu\text{-OH})-\text{Fe}^{III}$ cores, further supports this assignment.

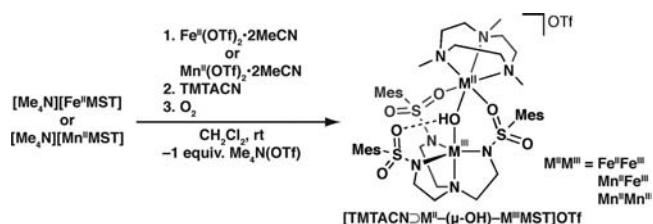
Transition-metal complexes with discrete dinuclear metal cores have important functional consequences in chemical and biological systems. In biology, several examples have been discovered in which both homo- and heterobimetallic centers are present within the active sites of proteins. Many metalloproteins, such as methanemmonoxigenase hydroxylase, hemerythrin, purple acid phosphatases, and ribonucleotide reductases (RNRs), utilize oxo- or hydroxo-bridged homobimetallic cores that contain Fe or Mn ions.¹ More recently, several classes of RNRs have been found to contain heterobimetallic MnFe cores.² These enzymes catalyze the reduction of nucleotides to 2'-deoxynucleotides via the activation of dioxygen or hydrogen peroxide and are known to play an essential role in nucleic acid metabolism.³ The function of most bimetallic active sites in metalloproteins often requires intermediates that contain an open coordination site for binding and activating small molecules.⁴

A variety of $M^{II}M^{III}$ bimetallic synthetic complexes that contain a bridging hydroxo or phenoxo group have been described previously. In many instances, these complexes utilize symmetric dinucleating ligands^{5–7} or form coordinatively saturated geometries around each metal center.^{8,9} We reported recently that the tetradentate sulfonamide-based tripodal ligand N,N',N'' -[2,2',2''-nitrilotris(ethane-2,1-diyl)]tris(2,4,6-trimethylbenzenesulfonamido) ($[\text{MST}]^{3-}$) enforces a five-coordinate geometry around a transition-metal center and contains a second metal-ion binding site to form heterobimetallic systems. Using this ligand, complexes with $[\text{M}^{II}-(\mu\text{-OH})-\text{M}^{III}]$ cores ($M^{II} = \text{Ca}, \text{Sr}, \text{Ba}; M^{III} = \text{Mn}, \text{Fe}$) were prepared from the activation of dioxygen.¹⁰ We have expanded the scope of our heterobimetallic systems to include two 3d transition-metal ions (Fe and Mn) in

which the metal centers are linked through a bridging hydroxo ligand and two sulfonamide groups of the $[\text{M}^{III}(\text{OH})\text{MST}]^-$ complex. The primary coordination sphere of the second metal ion is completed by 1,4,7-trimethyl-1,4,7-triazacyclononane (TMTACN) to form a six-coordinate metal center.

The preparation of $[\text{TMTACN}\supset\text{Mn}^{II}-(\mu\text{-OH})-\text{Fe}^{III}\text{MST}]^+$ (denoted as $[\text{Mn}^{II}(\text{OH})\text{Fe}^{III}]^+$) was achieved via the synthetic route outlined in Scheme 1. The visible absorbance spectrum of

Scheme 1. Preparative Route to $[\text{TMTACN}\supset\text{M}^{II}-(\mu\text{-OH})-\text{M}^{III}\text{MST}]^-$ Complexes



the isolated solid showed an absorbance band at $\lambda_{\text{max}} (\epsilon_{\text{M}}) = 390$ nm (4600) and a broad shoulder at 470 nm (1780 M) (Figure S1 in the Supporting Information, SI). A broad but intense band was observed in the Fourier transform infrared (FTIR) spectrum at 3244 cm^{-1} , which was assigned to the vibration of the O–H bond (Figure S2 in the SI).¹⁰ The broadness of this band suggests a strong intramolecular hydrogen bond between the hydroxo ligand and sulfonamide group. The formulation of the solid as $[\text{Mn}^{II}(\text{OH})\text{Fe}^{III}]^+$ was supported by electrospray ionization mass spectrometry (ESI-MS), in which the molecular weight and experimental isotope pattern matched those calculated for $[\text{Mn}^{II}(\text{OH})\text{Fe}^{III}]^+$ (Figure S3 in the SI). Using the same synthetic route, $[\text{TMTACN}\supset\text{Fe}^{II}-(\mu\text{-OH})-\text{Fe}^{III}\text{MST}]^+$ ($[\text{Fe}^{II}(\text{OH})\text{Fe}^{III}]^+$) and $[\text{TMTACN}\supset\text{Mn}^{II}-(\mu\text{-OH})-\text{Mn}^{III}\text{MST}]^+$ ($[\text{Mn}^{II}(\text{OH})\text{Mn}^{III}]^+$) were also prepared and characterized. These homobimetallic complexes served as control systems for $[\text{Mn}^{II}(\text{OH})\text{Fe}^{III}]^+$ and possessed properties expected for their formulation. For example, their ESI-MS spectra were consistent with those for homobimetallic complexes (Figure S3 in the SI). In addition, $[\text{Fe}^{II}(\text{OH})\text{Fe}^{III}]^+$ had an absorbance spectrum similar to that for $[\text{Mn}^{II}(\text{OH})\text{Fe}^{III}]^+$ with a peak at $\lambda_{\text{max}} = 387$ nm (6200), which appears to be representative

Received: June 29, 2013

Published: August 30, 2013

of complexes containing $[\text{Fe}^{\text{III}}(\text{OH})\text{MST}]^-$ units (Figure S1 in the SI).

The molecular structure of $[\text{Mn}^{\text{II}}(\text{OH})\text{Fe}^{\text{III}}]^+$ was determined by X-ray diffraction methods and revealed the expected heterobimetallic complex (Figure 1). The Fe^{III} and Mn^{II} centers

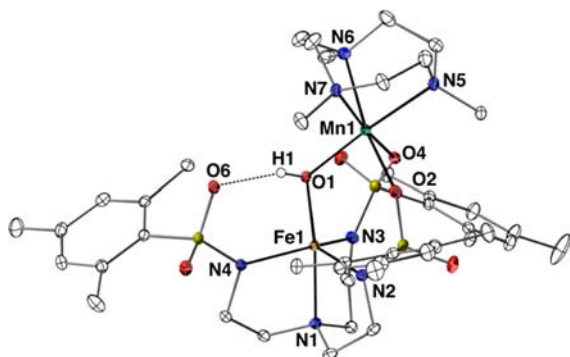


Figure 1. Thermal ellipsoid diagram depicting the molecular structure of $[\text{Mn}^{\text{II}}(\text{OH})\text{Fe}^{\text{III}}]^+$. Ellipsoids are drawn at the 50% probability level, and only the hydroxo H atom is shown for clarity. Selected bond lengths (Å): Fe1–O1, 1.888(1); Fe1–N1, 2.193(2); Fe1–N2, 2.030(2); Fe1–N3, 2.007(2); Fe1–N4, 2.036(2); Fe1...Mn1, 3.447(1); Mn1–O1, 2.048(1); Mn1–N5, 2.268(2); Mn1–N6, 2.276(2); Mn1–N7, 2.294(2); Mn1–O2, 2.196(1); Mn1–O4, 2.187(1); O1...O6, 2.646(2).

have different coordination geometries: the Fe^{III} center exhibits a five-coordinate, N_4O primary coordination sphere with a distorted trigonal-bipyramidal geometry. In contrast, the Mn^{II} center has a six-coordinate, N_3O_3 primary coordination sphere with a distorted octahedral geometry (Table S4 in the SI). Note that the configuration of the SO_2Ar groups produced a cavity that forms an intramolecular hydrogen bond between the $\text{Fe}^{\text{III}}\text{–OH–Mn}^{\text{II}}$ unit and O6 of the $[\text{MST}]^{3-}$ ligand with an O1...O6 distance of 2.646(2) Å. The molecular structures of the homobimetallic complexes $[\text{Fe}^{\text{II}}(\text{OH})\text{Fe}^{\text{III}}]^+$ and $[\text{Mn}^{\text{II}}(\text{OH})\text{Mn}^{\text{III}}]^+$ were also determined (Figures S4 and S5 in the SI) and used to support the assignment of $[\text{Mn}^{\text{II}}(\text{OH})\text{Fe}^{\text{III}}]^+$ as a heterobimetallic species (Table S4 in the SI). For instance, for the M^{II} center, the average $\text{M}^{\text{II}}\text{–N}_{\text{TMTACN}}$ bond distance is statistically the same in $[\text{Mn}^{\text{II}}(\text{OH})\text{Mn}^{\text{III}}]^+$ as it is in $[\text{Mn}^{\text{II}}(\text{OH})\text{Fe}^{\text{III}}]^+$ [2.277(7) vs 2.279(2) Å]; both values are significantly longer than the average bond distance of 2.210(2) Å observed in $[\text{Fe}^{\text{II}}(\text{OH})\text{Fe}^{\text{III}}]^+$. Moreover, the displacements of the M^{II} center from the plane formed by N5, N6, and N7 in $[\text{Mn}^{\text{II}}(\text{OH})\text{Mn}^{\text{III}}]^+$ and $[\text{Mn}^{\text{II}}(\text{OH})\text{Fe}^{\text{III}}]^+$ are nearly identical (1.557 vs 1.552 Å), while that found in $[\text{Fe}^{\text{II}}(\text{OH})\text{Fe}^{\text{III}}]^+$ is 1.471 Å. For the M^{III} center, the displacements of the M^{III} center from the plane formed by N2, N3, and N4 of $[\text{MST}]^{3-}$ are 0.359 Å in $[\text{Mn}^{\text{II}}(\text{OH})\text{Fe}^{\text{III}}]^+$ and 0.356 Å in $[\text{Fe}^{\text{II}}(\text{OH})\text{Fe}^{\text{III}}]^+$, yet in $[\text{Mn}^{\text{II}}(\text{OH})\text{Mn}^{\text{III}}]^+$, this displacement is only 0.286 Å.

Electron paramagnetic resonance (EPR) spectroscopy was used to further probe the properties of these complexes. For $[\text{Mn}^{\text{II}}(\text{OH})\text{Mn}^{\text{III}}]^+$, the EPR spectrum measured at 11 K displayed a signal from an $S = 1/2$ spin ground state of antiferromagnetically coupled Mn^{II} and Mn^{III} high-spin centers (Figure 2A). This signal displays an irregular pattern of hyperfine lines from the inequivalent nuclear spins of the two Mn centers. For $[\text{Fe}^{\text{II}}(\text{OH})\text{Fe}^{\text{III}}]^+$, the EPR spectrum measured at 11 K displayed a rhombic signal with g values of 1.91, 1.68, and 1.54 (Figure 2B). This type of spectrum is characteristic of complexes with an antiferromagnetically coupled $\text{Fe}^{\text{II}}\text{–}(\mu\text{-OH})\text{–Fe}^{\text{III}}$ core.^{5a} For both complexes, spin quantification of the spectra

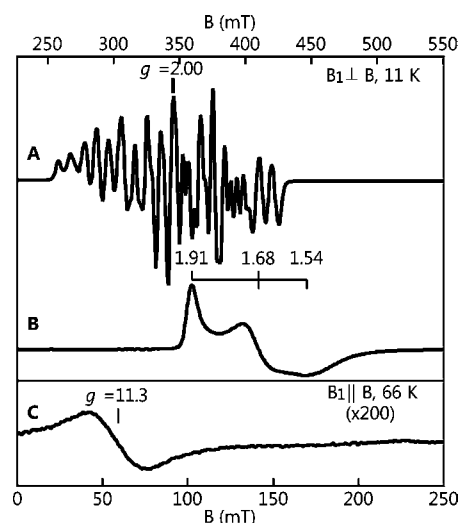


Figure 2. X-band EPR spectra for (A) $[\text{Mn}^{\text{II}}(\text{OH})\text{Mn}^{\text{III}}]^+$, (B) $[\text{Fe}^{\text{II}}(\text{OH})\text{Fe}^{\text{III}}]^+$, and (C) $[\text{Mn}^{\text{II}}(\text{OH})\text{Fe}^{\text{III}}]^+$.

indicated that the signals accounted for the amount of metal used in the reaction. No EPR signals were observed for $[\text{Mn}^{\text{II}}(\text{OH})\text{Fe}^{\text{III}}]^+$ at a temperature of 4 K. However, at higher temperatures (e.g., 66 K), a signal is observed at $g = 11.3$ for the microwave magnetic field oscillating parallel to the static magnetic field (Figure 2C). The absence of signals at low temperature and the presence of the parallel-mode signal at higher temperatures is consistent with antiferromagnetic coupling between the two d^5 metal centers in $[\text{Mn}^{\text{II}}(\text{OH})\text{Fe}^{\text{III}}]^+$. The observed antiferromagnetic coupling between the two metal centers is a key result that supports the persistence of the bimetallic complexes in solution.

The electrochemical results further support that the $[\text{M}^{\text{II}}(\text{OH})\text{M}^{\text{III}}]$ complexes are assembled in solution. The cyclic voltammogram for each complex exhibits two quasi-reversible one-electron redox processes that are assigned to the $\text{M}^{\text{II}}\text{M}^{\text{II}}/\text{M}^{\text{II}}\text{M}^{\text{III}}$ and $\text{M}^{\text{II}}\text{M}^{\text{III}}/\text{M}^{\text{III}}\text{M}^{\text{III}}$ couples (Figure 3). The most striking finding is that the two redox processes observed for the $[\text{Mn}^{\text{II}}(\text{OH})\text{Fe}^{\text{III}}]^+$ complex are nearly identical with the analogous redox process in the $[\text{Fe}^{\text{II}}(\text{OH})\text{Fe}^{\text{III}}]^+$ and $[\text{Mn}^{\text{II}}(\text{OH})\text{Mn}^{\text{III}}]^+$ complexes. Specifically, the $\text{Mn}^{\text{II}}\text{Fe}^{\text{II}}/\text{Mn}^{\text{II}}\text{Fe}^{\text{III}}$ couple at -0.88 V matches the $\text{Fe}^{\text{II}}\text{Fe}^{\text{II}}/\text{Fe}^{\text{II}}\text{Fe}^{\text{III}}$ couple

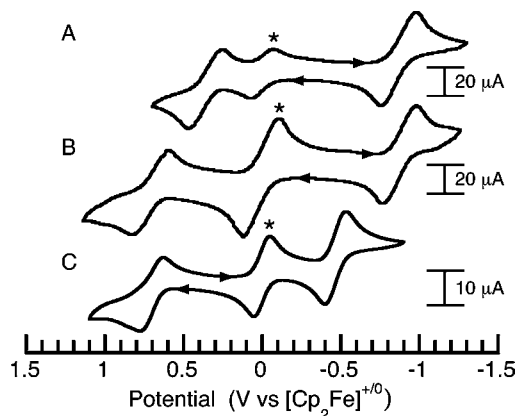


Figure 3. Cyclic voltammograms of (A) $[\text{Fe}^{\text{II}}(\text{OH})\text{Fe}^{\text{III}}]^+$, (B) $[\text{Mn}^{\text{II}}(\text{OH})\text{Fe}^{\text{III}}]^+$, and (C) $[\text{Mn}^{\text{II}}(\text{OH})\text{Mn}^{\text{III}}]^+$ measured in CH_2Cl_2 (0.1 M TBAP). The cyclic voltammograms in parts A and B were collected at 100 mV s^{-1} and that in part C at 20 mV s^{-1} in the presence of $[\text{Cp}_2\text{Fe}]^+$ (*).

at -0.87 V, while the $\text{Mn}^{\text{II}}\text{Fe}^{\text{III}}/\text{Mn}^{\text{III}}\text{Fe}^{\text{III}}$ couple at 0.71 V matches the $\text{Mn}^{\text{II}}\text{Mn}^{\text{III}}/\text{Mn}^{\text{III}}\text{Mn}^{\text{III}}$ couple at 0.71 V. These results indicate that the Mn^{II} ion resides in the [TMTACN] binding site and the Fe^{III} center is coordinated to the $[\text{MST}]^{3-}$ ligand. Furthermore, the separations between the first and second redox processes in the $[\text{M}^{\text{II}}(\text{OH})\text{M}^{\text{III}}]^+$ systems are extremely large, with differences of 1.59 , 1.23 , and 1.18 V for the $[\text{Mn}^{\text{II}}(\text{OH})\text{Fe}^{\text{III}}]^+$, $[\text{Fe}^{\text{II}}(\text{OH})\text{Fe}^{\text{III}}]^+$, and $[\text{Mn}^{\text{II}}(\text{OH})\text{Mn}^{\text{III}}]^+$ complexes. These separations suggest that the mixed-valence $[\text{M}^{\text{II}}(\text{OH})\text{M}^{\text{III}}]^+$ species should be relatively stable toward disproportionation.^{5–8}

In summary, we have described the preparation and properties of a series of hetero- and homobimetallic complexes of Fe and Mn ions in differing coordination environments. Structural studies confirmed that each complex contains a $\text{M}^{\text{II}}-(\mu\text{-OH})-\text{M}^{\text{III}}$ core, with the hydroxo ligand also forming an intramolecular hydrogen bond with the $[\text{MST}]^{3-}$ ligand. The metal-ion cores adopt stable mixed-valent states of $\text{Mn}^{\text{II}}\text{Fe}^{\text{III}}$, $\text{Fe}^{\text{II}}\text{Fe}^{\text{III}}$, and $\text{Mn}^{\text{II}}\text{Mn}^{\text{III}}$, whose assignments are supported by EPR results that are consistent with antiferromagnetic coupling of the spins through the hydroxo unit. In addition, two quasi-reversible one-electron redox processes corresponding to the $\text{M}^{\text{II}}\text{M}^{\text{III}}/\text{M}^{\text{II}}\text{M}^{\text{III}}$ and $\text{M}^{\text{II}}\text{M}^{\text{III}}/\text{M}^{\text{III}}\text{M}^{\text{III}}$ couples were clearly observed with all of the $[\text{M}^{\text{II}}(\text{OH})\text{M}^{\text{III}}]^+$ systems via cyclic voltammetry. These results further illustrate the ability of tripodal sulfonamido ligands to form discrete bimetallic complexes.

■ ASSOCIATED CONTENT

■ Supporting Information

Crystallographic data in CIF format, experimental details, and UV–vis, FTIR, and ESI-MS spectra for all complexes. This material is available free of charge via the Internet at <http://pubs.acs.org>.

■ AUTHOR INFORMATION

Corresponding Author

*E-mail: aborovik@uci.edu.

Notes

The authors declare no competing financial interest.

■ ACKNOWLEDGMENTS

We thank the NIH (Grant GM050781 to A.S.B.; Grant GM77387 to M.P.H.) for financial support of this work.

■ REFERENCES

- (1) (a) Kurtz, D. M. *Chem. Rev.* **1990**, *90*, 585. (b) Wu, A. J.; Penner-Hahn, J. E.; Pecoraro, V. L. *Chem. Rev.* **2004**, *104*, 903 and references cited therein. (c) Schenk, G.; Mitic, N.; Gahan, L. R.; Ollis, D. L.; McCearry, R. P.; Guddat, L. W. *Acc. Chem. Res.* **2012**, *45*, 1593.
- (2) (a) Jiang, W.; Yun, D.; Saleh, L.; Barr, E. W.; Xing, G.; Hoffart, L. M.; Maslak, M. A.; Krebs, C.; Bollinger, J. M. *Science* **2007**, *316*, 1188. (b) Andersson, C. S.; Høgbom, M. *Proc. Natl. Acad. Sci. U.S.A.* **2009**, *106*, 5633. (c) Dassama, L. M. K.; Boal, A. K.; Krebs, C.; Rosenzweig, A. C.; Bollinger, J. M., Jr. *J. Am. Chem. Soc.* **2012**, *134*, 2520.
- (3) (a) Cotruvo, J. A., Jr.; Stubbe, J. *Annu. Rev. Biochem.* **2011**, *80*, 733. (b) Tomter, A. B.; Zoppellaro, G.; Andersen, N. H.; Hersleth, H.-P.; Hammerstad, M.; Røhr, Å. K.; Sandvik, G. K.; Strand, K. R.; Nilsson, G. E.; Bell, C. B., III; Barra, A.-L.; Blasco, E.; Le Pape, L.; Solomon, E. I.; Andersson, K. K. *Coord. Chem. Rev.* **2013**, *257*, 3 and references cited therein.
- (4) (a) Das, D.; Eser, B. E.; Han, J.; Sciore, A.; Marsh, E. N. G. *Angew. Chem., Int. Ed.* **2011**, *50*, 7148. (b) Hayashi, T.; Caranto, J. D.; Matsumura, H.; Kurtz, D. M., Jr.; Moënné-Loccoz, P. *J. Am. Chem. Soc.* **2012**, *134*, 6878.
- (5) (a) Borovik, A. S.; Que, L.; Papaefthymiou, V.; Muenck, E.; Taylor, L. F.; Anderson, O. P. *J. Am. Chem. Soc.* **1988**, *110*, 1986. (b) Buchanan, R. M.; Mashuta, M. S.; Richardson, J. F.; Webb, R. J.; Oberhausen, K. J.; Nanny, M. A.; Hendrickson, D. N. *Inorg. Chem.* **1990**, *29*, 1299.
- (6) (a) Borovik, A. S.; Papaefthymiou, V.; Taylor, L. F.; Anderson, O. P.; Que, L. *J. Am. Chem. Soc.* **1989**, *111*, 6183. (b) Bossek, U.; Hummel, H.; Weyhermüller, T.; Bili, E.; Wieghardt, K. *Angew. Chem., Int. Ed. Engl.* **1996**, *34*, 2642.
- (7) (a) Diril, H.; Chang, H. R.; Zhang, X.; Larsen, S. K.; Potenza, J. A.; Pierpont, C. G.; Schugar, H. J.; Isied, S. S.; Hendrickson, D. N. *J. Am. Chem. Soc.* **1987**, *109*, 6207. (b) Bossek, U.; Hummel, H.; Weyhermüller, T.; Wieghardt, K.; Russell, S.; van der Wolf, L.; Kolb, U. *Angew. Chem., Int. Ed. Engl.* **1996**, *35*, 1552.
- (8) (a) Kanda, W.; Moneta, W.; Bardet, M.; Bernard, E.; Debaecker, N.; Laugier, J.; Bousseksou, A.; Chardon-Noblat, S.; Latour, J.-M. *Angew. Chem., Int. Ed. Engl.* **1995**, *34*, 588. (b) Smith, S. J.; Riley, M. J.; Noble, C. J.; Hanson, G. R.; Stranger, R.; Jayaratne, V.; Cavigliasso, G.; Schenk, G.; Gahan, L. R. *Inorg. Chem.* **2009**, *48*, 10036. (c) Carboni, M.; Clémancey, M.; Molton, F.; Pécaut, J.; Lebrun, C.; Dubois, L.; Blondin, G.; Latour, J. M. *Inorg. Chem.* **2012**, *51*, 10447.
- (9) For examples of unsymmetrical heterobimetallic complexes, see: (a) Neves, A.; Lanznster, M.; Bortoluzzi, A. J.; Perlta, R. A.; Castllano, E. E.; Herrald, P.; Riley, M. J.; Schenk, G. *J. Am. Chem. Soc.* **2007**, *129*, 7486. (b) de Souza, B.; Kreft, G. L.; Bortolotto, T.; Ternzi, H.; Bortoluzzi, A. J.; Castllano, E. E.; Perlta, R. A.; Domingos, J. B.; Neves, A. *Inorg. Chem.* **2013**, *52*, 3594.
- (10) (a) Park, Y. J.; Ziller, J. W.; Borovik, A. S. *J. Am. Chem. Soc.* **2011**, *133*, 9258. (b) Park, Y. J.; Cook, S. A.; Sickerman, N. S.; Sano, Y.; Ziller, J. W.; Borovik, A. S. *Chem. Sci.* **2013**, *4*, 717.